

2015

# Design of Dressed Crab Cavities for the HL-LHC Upgrade

C. Zanoni

K. Artoos


S. Atieh

I. Aviles-Santillana

S. Belomestnykh

*See next page for additional authors*

Follow this and additional works at: [https://digitalcommons.odu.edu/physics\\_fac\\_pubs](https://digitalcommons.odu.edu/physics_fac_pubs)

 Part of the [Engineering Physics Commons](#), and the [Plasma and Beam Physics Commons](#)

---

## Repository Citation

Zanoni, C.; Artoos, K.; Atieh, S.; Aviles-Santillana, I.; Belomestnykh, S.; Ben-Zvi, I.; Brachet, J.P.; Burt, G.; Calaga, R.; Captina, O.; De Silva, S. U.; Delayen, J. R.; May, A.; Marinov, K.; Olave, R.; Park, H.; and Templeton, N., "Design of Dressed Crab Cavities for the HL-LHC Upgrade" (2015). *Physics Faculty Publications*. 266.

[https://digitalcommons.odu.edu/physics\\_fac\\_pubs/266](https://digitalcommons.odu.edu/physics_fac_pubs/266)

## Original Publication Citation

Zanoni, C., Artoos, K., Atieh, S., Aviles Santillana, I., Belomestnykh, S., Ben-Zvi, I... & Capelli, T. (2015, December). Design of Dressed Crab Cavities for the HL-LHC Upgrade. In *Proceedings of the 17th International Conference on RF Superconductivity (SRF2015)*, Whistler, BC, Canada, Sept. 13-18, 2015 (pp. 1284-1288).

---

**Authors**

C. Zanoni, K. Artoos, S. Atieh, I. Aviles-Santillana, S. Belomestnykh, I. Ben-Zvi, J.P. Brachet, G. Burt, R. Calaga, O. Captina, S. U. De Silva, J. R. Delayen, A. May, K. Marinov, R. Olave, H. Park, and N. Templeton

## DESIGN OF DRESSED CRAB CAVITIES FOR THE HL-LHC UPGRADE\*

C. Zanoni<sup>†1</sup>, K. Artoos<sup>1</sup>, S. Atieh<sup>1</sup>, I. Aviles Santillana<sup>1,2</sup>, S. Belomestnykh<sup>3,4</sup>, I. Ben-Zvi<sup>3,4</sup>, J.-P. Brachet<sup>1</sup>, G. Burt<sup>5</sup>, R. Calaga<sup>1</sup>, O. Capatina<sup>1</sup>, T. Capelli<sup>1</sup>, F. Carra<sup>1</sup>, L. Dassa<sup>1</sup>, S.U. De Silva<sup>6</sup>, J. Delayen<sup>6</sup>, G. Favre<sup>1</sup>, P. Freijedo Menendez<sup>1</sup>, M. Garlaschè<sup>1</sup>, M. Guinchard<sup>1</sup>, T. Jones<sup>7</sup>, N. Kuder<sup>1</sup>, S. Langeslag<sup>1</sup>, R. Leuxe<sup>1</sup>, Z. Li<sup>8</sup>, A. May<sup>6</sup>, K. Marinov<sup>6</sup>, T. Nicol<sup>9</sup>, R. Olave<sup>6</sup>, H. Park<sup>6</sup>, S. Pattalwar<sup>7</sup>, L. Prever-Loiri<sup>1</sup>, A. Ratti<sup>10</sup>, N. Templeton<sup>6</sup>, G. Vandoni<sup>1</sup>, S. Verdú-Andres<sup>3</sup>, Q. Wu<sup>3</sup>, and B. Xiao<sup>3</sup>

<sup>1</sup>CERN, Geneva, Switzerland

<sup>2</sup>University Carlos III, 28911 Madrid, Spain

<sup>3</sup>BNL, Upton, NY 11973, USA

<sup>4</sup>Stony Brook University, Stony Brook, NY 11794, USA

<sup>5</sup>Cockcroft Institute, Lancaster University, UK

<sup>6</sup>Old Dominion University, Norfolk, VA, 23529, USA

<sup>7</sup>STFC Daresbury Laboratory, UK

<sup>8</sup>SLAC, Menlo Park, CA 94025, USA

<sup>9</sup>Fermilab, Batavia, IL 60510, USA

<sup>10</sup>LBNL, Berkeley, CA 94707, USA

### Abstract

RF crab cavities are one of the key systems for the HL-LHC (High Luminosity LHC) upgrade. In view of extensive tests with beam in the SPS, two cavity concepts for the design of such systems are being developed: the Double Quarter Wave (DQW) and the RF Dipole (RFD).

Cavities built out of thin niobium plates require external stiffeners in order to sustain the loads applied through their lifetime. Adequate cooling and efficient magnetic shielding are necessary to reach the required kick gradients and maintain the performance. To minimize the deformation of the cavity during assembly and operation, a design of the helium tank with bolts, for structural strength, and superficial welds, to guarantee vacuum integrity, is proposed. This approach, which is a non standard practice for helium tanks, will be reviewed in this paper.

### INTRODUCTION

The statistical gain obtained by running LHC after 2020 with the current performance is marginal [1]. Thus, in order to keep LHC at the forefront of physics, a significant luminosity increase is foreseen through the HL-LHC upgrade. The crab cavities are among the critical systems required for obtaining the desired new performance.

Similar devices have already been employed at KEK [2]. However, the use of elliptical shape cavities poses major space and integration issues. This determines the need for a wholly new design. Two concepts are under development through CERN and the USLARP consortium: the Double Quarter Wave (DQW) and the RF Dipole (RFD), [3–5]. The

RF design is finalized while the detailed engineering phase is underway.

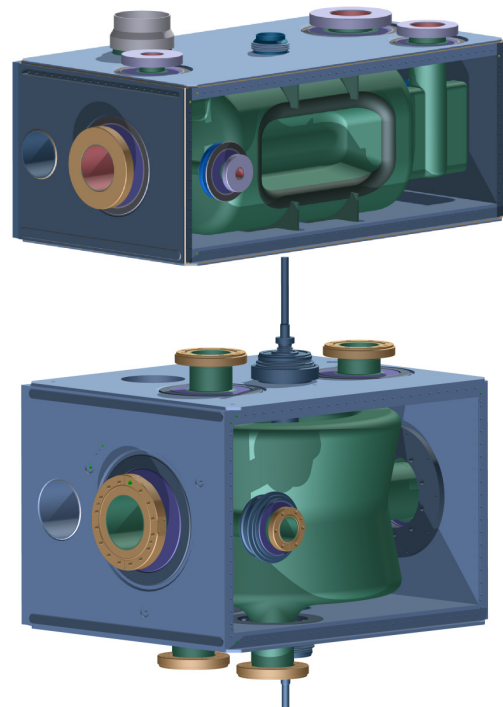


Figure 1: 3D views of the RFD (top) and DQW (bottom) dressed cavities.

The cavities are built out of niobium plates. In order to minimize the change in frequency due to fluctuations in external pressure<sup>1</sup> and allow some margin on the temperature

\* The research leading to these results has received funding from the European Commission under the FP7 project HiLumi LHC, GA no. 284404, co-funded by the DoE, USA and KEK, Japan

<sup>†</sup> carlo.zanoni@cern.ch

<sup>1</sup> superfluid helium at 2 K operates at 20 mbara  $\pm$  1 mbara, while helium at 4 K at 1.3  $\pm$  0.1 bara

before a quench, a saturated bath of superfluid helium at 2 K will be used for cooling down.

For operating the cavity within the required environment and guarantee thermal and magnetic insulation a large set of systems is needed. The ensemble is referred to as cryomodule. The heart of the cryomodule is the dressed cavity, that provides confinement of liquid helium, gives mechanical support to the cavity, contains a first magnetic shield. On top of that, the dressed cavity interfaces with the continuous beamline, with power and HOM couplers, tuner, cryogenics and with the cryomodule. Main scope of this paper is to describe the helium tank design and fabrication strategy and the related numerical simulations. The magnetic shield design strategy will also be briefly described. HOM couplers, tuning system, magnetic shielding along with the cryomodule current design are treated elsewhere in this conference [6–8].

Although in steady-state operation at 2 K the saturated liquid helium pressure (20 mbara) is not significantly loading the cavity, during cool-down pressure may rise to about 1.8 bara. In order to guarantee fast heat evacuation in case of local quench, the cavity walls are 4 mm thick niobium sheets, which are not sufficient to withstand such pressure. Therefore, the helium tank also plays a role as stiffener of the cavity itself.

### The Helium Tank

Two materials have been considered for the helium tanks: stainless steel and titanium. Stainless steel (AISI 316LN, non-magnetic) is well known and is easily machinable. On the other hand, titanium has roughly the same thermal contraction as niobium (in the order of 1.5 mm/m from 300 K to 2 K), while the contraction of stainless steel is twice as large and leads to large stresses. Titanium grade 2 is therefore chosen as material for the helium tank, after several simulations.

The helium tank is designed as a cavity stiffener, in particular during peak pressure loading and tuning, and is designed to limit the maximum stress on the cavity. In fact, the tank deformation directly determines the stress distribution on the cavity. The initial tank design was based on a fully welded concept and was discarded due to high deformations after welding. It was estimated - see Fig. 2 for test piece - that 3 mm weld seams would result in a 1 mm distortion at the interface with the cavity. The quality of the welds would also not be optimal.

In the final designs, Fig. 1, the tanks are boxes assembled from 6 plates held together by a large set of screws (ISO M6). Welds at the plates interfaces guarantee leak tightness. Small covers are employed on top of the screws for the same reasons.

## CALCULATION OF THE MECHANICAL PERFORMANCE

The bolted design with leak-tight welds is uncommon, therefore calculations are performed for the very worst-case

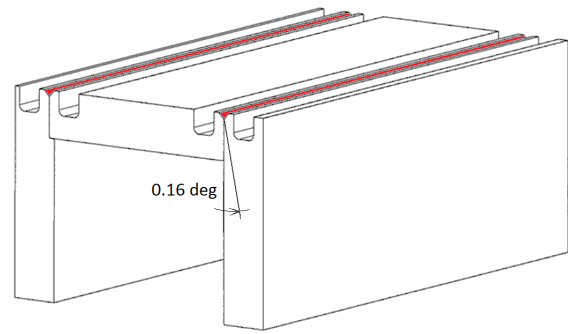


Figure 2: Test piece for estimation of weld distortion. The angular dimension is the most critical.

scenario. The behavior of the bolts, along with the forces on the welds and the stress on tank and cavity, are examined using ANSYS15. Reaction forces and moments are extracted from the numerical calculations and used to perform further calculations, where needed. The final assessment of the helium tank includes the verification of the bare cavity along with all the bolts and welds.

### Main Assumptions and Load Cases

The most demanding load case happens at room temperature, when niobium has a low yield strength, and is shown in Table 1. Other less critical load cases are encountered during the tank/cavity lives, such as the normal operation, in which pressure is negligible. All these cases are evaluated.

Table 1: Most Demanding Set of Loads Applied to the Dressed Cavities

Type	Value
Temperature	300 K (i.e. no gradient)
Bolt preload	4500 N
Gravity	9806.6 mm/s <sup>2</sup>
Pressure	0.18 MPa
Pre-tuning	0.12 mm (only for DQW cavity center)

In order to perform a worst-case evaluation, it is assumed that there is no friction between the tank plates and that all the load is carried by the bolted joints and welds.

A full model of helium tank and cavity is examined. The levels of stress and deformation are verified according to the standard EN13445-3 [9], that applies to pressure equipment. A sub-model is employed for the cavity, in order to limit the nodes in the FE analysis.

Helium tank plates are fastened using bolts evenly distributed along 12 edges. Bolts must limit the load carried by the weld, which must continuously be leak tight, and are modeled as beam lines (Fig. 3) according to VDI 2230:2 [10], with cross section properties according to the same standard. The beam length is represented as the distance between the bolt head and the beginning of the thread in the plates. The beam top and bottom nodes are coupled respectively with the projected head face and threaded hole. Titanium grade 5 is selected as bolt material, because of

its high proof stress and a coefficient of thermal expansion almost identical to titanium grade 2.

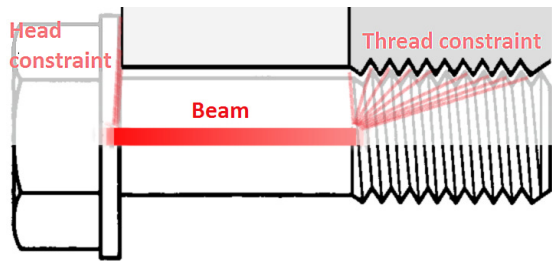


Figure 3: Model of the bolts for FE calculations. The screw is modeled by a beam constrained at both extremities. The length of the beam reflects the part of bolt actually under load. In fact, it is well known that only the first 2 - 3 threads are actually carrying loads.

The bolts experience several loads. The axial tensile force consists of the preload, the direct effect of pressure and the prying force. That force is generated as a result of the local rotation of the cover plates around the external edge. The shear force is an outcome of the relative movement of the plates that also generates a bending moment. The torsional moment is due to the preload in the bolts, applied through a torque. The stress is finally extracted from the combination of these forces/moments and is compared with the allowable value.

Although the function of the welds is not structural, the reaction moments and forces are carried in part by them and a strength assessment is required to check their performance. The calculations are based on the assumption of a uniform distribution of the loads through the weld length. The welds are treated as lines and modeled as edge-to-face bonded contacts. In the simulation, these internal contacts become active after the bolt preload is applied, in order to avoid constraints in such a phase, as it happens in the real world.

**Results, Bolts and Weld Seams Assessment**

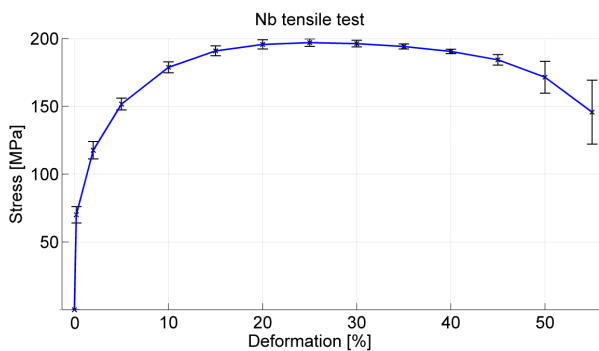


Figure 4: Characterization of niobium used for cavities production, with uncertainty.

In general, the stress on the helium tank appears to be low, Fig. 5 and 6. The maximum allowable stress is 275 MPa, which is above the highest values found in the simu-

lations even considering the 1.5 factor needed in pressure equipments [9].

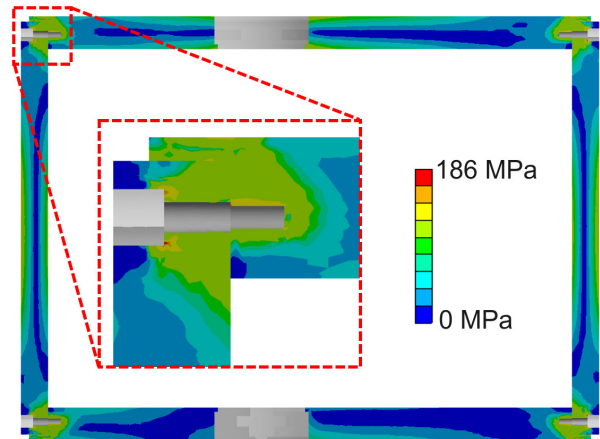


Figure 5: Stress through a plane in the middle of the tank. The values around the bolt head are an effect of numerical errors.

The stress on the cavity is as high as the elastic limit, Fig. 7, which is equal to 75 MPa. However, the rupture limit is much higher, Fig. 4. The limit becomes 50 MPa applying the 1.5 factor required by [9]. The analysis of the linearized stress according to the standards suggests that these values are all acceptable. On top of that, the safety of the values obtained is confirmed by elasto-plastic analysis, not discussed here.

The continuity of contact between the plates is also a requirement. All the interfaces show a satisfactory behaviour such that of Fig. 6: the contact pressure is always above zero for at least a part of the thickness (small dimension).

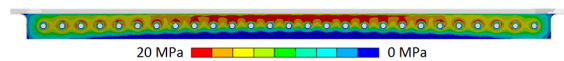


Figure 6: Contact between plates.

The maximum values of the loads in the bolts are shown in Table 2 and are extracted from two different models. The first one constrains the plates only with the bolts, therefore neglecting the effect of the welds. The second one has both bolts and welds, instead. This allows checking the safety coefficients for the stand-alone performance of the bolts along with the effect of the welded joints.

The calculations show that the bending moments and shear forces heavily contribute to the high stress level of the bolts. It is worth reminding that friction between plates, whose value is highly uncertain, is here neglected. According to these analyses, the safety coefficient is acceptable in these conditions even following a worst-case approach. The reaction forces/moments are extracted and used to calculate the equivalent stress.

The welds are subjected to the complex load condition including bending and torsion. The analysis of an individual weld group is subdivided into FE calculation for a simplified representation of the weld and an analytic calculation



Figure 7: Stress on DQW (top) and RFD (bottom) cavities. The red locations require a further step in the assessment with the linearized stress.

Table 2: Stress Estimated on the Bolts for the DQW

	Units	Bolts	Bolts + Welds
Peak Stress	$\sigma_{eq}$ [MPa]	620	480
Allowable Stress (Ti grade 2)	$S_p$ [MPa]		830
Safety Factor	$k$	1.34	1.74

based on data extracted from the FE results. The estimated stress is an average value, whereas the peak stress can be significantly higher. However, the peak would be localized and would matter only in case of fatigue, which is not an issue for the helium tank. Figure 8 shows the margin factor (with respect to an allowable value of 280 MPa for Ti grade 2) for the main welds. Equivalent calculation is performed for all the welds such as the ones that block the cover above the screws.

### MAGNETIC SHIELDING

A well known source of losses [11] in an RF cavity is the trapped DC magnetic field. For the crab cavities a two-layer solution is foreseen. One layer will be outside the pair of dressed cavities and the other will be inside each of the helium tanks. The internal one is a 1 mm thick Cryophy™. Figure 9 shows the overall results in terms of magnitude for the worst case field direction.

Mechanical stresses can dramatically alter the shielding performance. In order to mitigate this effect, particular care has to be taken during assembly and the constraining sys-

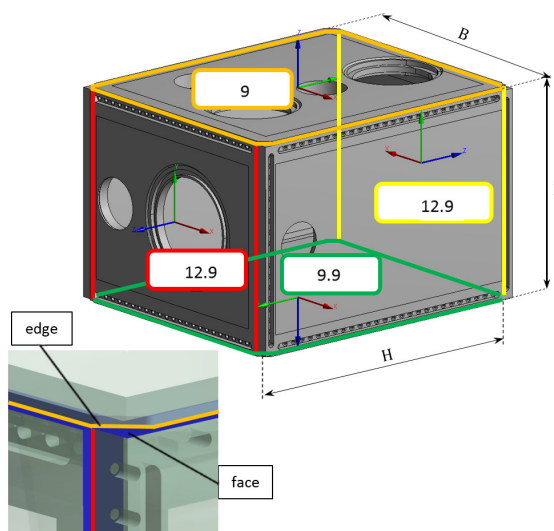


Figure 8: Margin factor (with respect to an allowable value of 280 MPa for Ti grade 2) for the main welds.

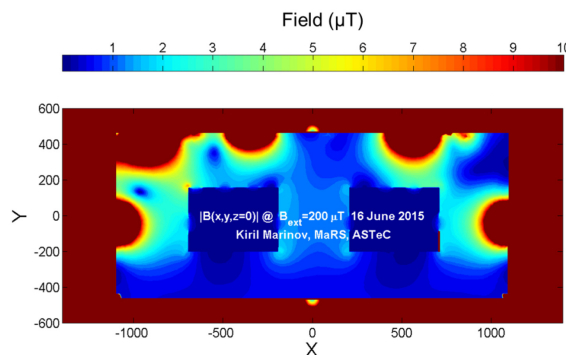


Figure 9: Magnetic field amplitude inside the cryomodule, scale 0 to 10  $\mu T$  (top). An external field of 200  $\mu T$  in the direction parallel to X (longitudinal) is applied.

tem must allow enough flexibility to accommodate thermal contraction. Before that, some simple tests are planned for characterizing the bolts in different load conditions.

### PROTOTYPE MODEL FOR TESTS

In order to qualify the design concept of the helium tank, validate the calculations and test the mounting and assembly procedure, a prototype of the vessel was designed and machined and is currently (September 2015) being assembled. Such a system resembles the helium tank for most of its features, Fig. 10, but it contains no cavity. The ports for the couplers are substituted with flanges, which allow wires feed-throughs or vacuum/pressure pumping. The openings for cryo, pick-up and tuner are replaced by blind holes. The thickness of the residual material is roughly tuned to allow a local deformation comparable to the deformation estimated on the real tank. In fact, the use of blind holes increases the total force applied on the plate, but also increases the stiffness. Finally, part of titanium of the plates is removed in order to reduce the mass. It is worth noting that eventually

such material will be removed on the internal side of the final tank instead than on the external.



Figure 10: Prototype model of the helium tank.

Currently, 3 main test steps are foreseen and under preparation:

- Mounting and welding.
- Pressure test. This test is performed at  $\Delta p = 2.6 \text{ bar}$  and at room temperature. It has been estimated that the combination of volume (70 l) and pressure is equivalent to the energy of 4 g of TNT. The test will be performed in a bunker, although the stored energy is low and does not raise safety concerns. Finally, the use of gas is preferred to liquid to avoid the subsequent drying procedure.
- Cold-shock test. The tank is cooled from room temperature to 80 K by immersion in liquid Nitrogen for 5 cycles. The cool-down time is between 30 and 60 min. The warm-up takes a few hours and requires a hot air supply. Inside the tank, vacuum is pumped in order to avoid formation of ice and allow leak tightness tests between cycles.

After mounting, welding and each of the tests, a full dimensional control and leak tightness test will be performed.

Indeed, the first goal is to prove that the tank can survive these conditions as well as remain leak tight. Moreover, the stress on specific location of the plates will be measured along with the total deformation at the virtual beam axis interfaces and bolts preload and compared with the FE results. Both a model with frictionless contact and one with a small (0.3) friction coefficient have been considered. They show that the maximum stress on the bolts decreases from 655 MPa to 452 MPa. It is expected that the real behavior is closer to the model that takes friction into account.

## CONCLUSIONS

RF compact crab cavities are one of the key systems for increasing the LHC luminosity through the HL-LHC upgrade. These devices, developed in two parallel concepts, have already been through a successful RF design. Correct operation of the cavities requires a large set of auxiliary systems. The core of these systems is the so called dressed cavity which includes the helium tank and the magnetic shielding. According to simulations, the approach followed for the tank design guarantees a safe operation even in worst-case load conditions. Extensive tests for design, fabrication and assembly validation are in preparation and will start soon. In particular, a full prototype of the tank was machined, is being assembled and will be tested under representative loads.

## REFERENCES

- [1] G. Apollinari, O. Brüning and L. Rossi, "High Luminosity LHC Project Description", CERN-ACC-2014-0321, Geneva, December 2014. <http://cds.cern.ch/record/1974419>
- [2] K. Hosoyama et al., "Development of the KEK-B Superconducting Crab Cavity", EPAC'08, Genova, Italy, 2008, HXM02.
- [3] S.U. De Silva et al., "Electromagnetic Design of 400 MHz RF-Dipole Crabbing Cavity for LHC High Luminosity Upgrade", THPB053, *These Proceedings*, SRF'15, Whistler, Canada (2015).
- [4] B. Xiao et al., "Design, prototyping, and testing of a compact superconducting double quarter wave crab cavity", *Physical Review Special Topics* 18 (4), 2015.
- [5] Q. Wu, "Crab cavities: Past, present, and future of a challenging device", IPAC15, Richmond, USA, 2015.
- [6] C. Zaroni et al., "Engineering Design and Prototype Fabrication of HOM Couplers for HL-LHC Crab Cavities", THPB069, *These Proceedings*, SRF'15, Whistler, Canada (2015).
- [7] K. Artoos et al., "Development of SRF Cavity Tuners for CERN", THPB060, *These Proceedings*, SRF'15, Whistler, Canada (2015).
- [8] F. Carra et al., "Crab Cavity and Cryomodule Development for HL-LHC", FRBA02, *These Proceedings*, SRF'15, Whistler, Canada (2015).
- [9] VV.AA., "EN 13445-3", Paris, 2008.
- [10] VV.AA., "VDI 2230", Berlin, 2014.
- [11] H. Padamsee, "RF superconductivity: science, technology, and applications", 2nd ed., Wiley, New York, 2009.